Interfaces and Free Boundaries **19** (2017), 553–570
DOI 10.4171/IFB/392

A conservative scheme for non-classical solutions to a strongly coupled PDE-ODE problem

C. CHALONS
Laboratoire de Mathématiques de Versailles, UVSQ, CNRS, Université Paris-Saclay, 78035 Versailles, France
E-mail: christophe.chalons@uvsq.fr

M. L. DELLE MONACHE
Rutgers University – Camden, USA, and Inria, Univ. Grenoble Alpes, CNRS, GIPSA-lab, 38000 Grenoble, France
E-mail: ml.dellemonache@inria.fr

P. GOATIN
Inria Sophia Antipolis – Méditerranée, Université Côte d'Azur, Inria, CNRS, LJAD, 2004 route des Lucioles – BP 93, 06902 Sophia Antipolis Cedex, France
E-mail: paola.goatin@inria.fr

[Received 11 December 2015 and in revised form 24 January 2017]

We consider a strongly coupled PDE-ODE system modeling the influence of a slow and large vehicle on road traffic. The model consists of a scalar conservation law describing the main traffic evolution and an ODE accounting for the trajectory of the slower vehicle that depends on the downstream traffic density. The moving constraint is operated by an inequality on the flux, which accounts for the bottleneck created on the road by the presence of the slower vehicle. We introduce a conservative scheme for the constrained hyperbolic PDE and we use a tracking algorithm for the ODE. We perform numerical tests and compute numerically the order of convergence.

2010 Mathematics Subject Classification: Primary 35L65; Secondary 90B20.

Keywords: Scalar conservation laws with local moving constraints, traffic flow modeling, PDE-ODE coupling, conservative finite volume schemes.

1. Introduction

The problem considered in this paper is a coupled model consisting of a partial differential equation (PDE) and an ordinary differential equation (ODE). The coupled PDE-ODE model describes a large, slow moving vehicle (that we will refer to as "the bus") interacting with the surrounding traffic flow, generating a moving bottleneck. The Lighthill-Whitham-Richards (LWR) [36, 37] model (i.e., a scalar conservation law) is used to describe the evolution in time of the mean traffic density on a road, while an ODE accounts for the slower vehicle trajectory. The loss of road capacity due to the presence of the bus is expressed by an inequality constraint on the vehicles flow at the bus position.

The model was first introduced and studied in an engineering setting [26, 33] (see also [18, 19] for a numerical treatment). A rigorous mathematical framework and an existence result were later proposed in [21]. Other models for moving bottlenecks on roads are proposed in the applied mathematics literature: in [25, 32] the flux constraint is modeled by a mollifier, thus preserving the

smoothness of the flux function; a 2×2 system modeling traffic flow coupled with a second order ODE is presented in [5]. In these works, standard numerical methods can be applied.

Conservation laws with locally constrained flux function were first introduced in [16] to model fixed constraints like toll gates. Well-posedness results in the BV and $\mathbf{L}^\infty$ settings, as well as the convergence of adapted finite volume schemes are given in [4, 16]. Extensions to non-concave fluxes and systems were also proposed in [14] and [23] respectively. In those papers, anyway, the constraint position is fixed, and the analytical and numerical treatments are therefore easier than in the present case. In particular, no stability result with respect to initial data is currently available for the PDE-ODE system considered in this paper.

A first numerical strategy to compute approximate solutions was proposed in [20], based on locally non-uniform moving meshes to track the bus position, which captures exactly non-classical discontinuities but may result in complex coding procedures.

In this paper we follow another approach to avoid non-uniform moving meshes. The main point here is related to the presence of non-classical shocks in the solutions of the model under consideration. It is well-known that, in this context, standard conservative finite volume methods cannot be applied and fail in producing good numerical results. Glimm's scheme can be used but it is not strictly conservative. In order to obtain a numerical scheme which is conservative on fixed meshes and able to compute non-classical solutions, we propose to adapt to the present context of strongly coupled PDE-ODE system a reconstruction strategy approach introduced in [7] for scalar conservation laws and extended to systems by [1–3]. This technique allows to precisely capture moving non-classical discontinuities on fixed meshes still guaranteeing conservation, unlike Glimm's scheme. An important feature of the proposed method is to be exact for isolated classical and non-classical shocks, which means in particular only one point of numerical diffusion (on each cell the approximate value corresponds to the value of the average of the exact solution). In the general case, shocks are still computed without numerical diffusion and convergence is proved numerically. So far, however, no rigorous convergence result is available. Several test cases, some of them being significant from the modeling point of view, are proposed to illustrate these features.

2. Mathematical model

The coupled PDE-ODE model in [21] reads

$$\begin{cases} \partial_t \rho + \partial_x f(\rho) = 0, & (t,x) \in \mathbb{R}^+ \times \mathbb{R}, \quad (2.1a) \\ \rho(0,x) = \rho_0(x), & x \in \mathbb{R}, \quad (2.1b) \\ f\Big(\rho\big(t,y(t)\big)\Big) - \dot{y}(t)\rho\big(t,y(t)\big) \leqslant \dfrac{\alpha R}{4V}\big(V - \dot{y}(t)\big)^2 & t \in \mathbb{R}^+, \quad (2.1c) \\ \dot{y}(t) = \omega\Big(\rho\big(t,y(t)+\big)\Big), & t \in \mathbb{R}^+, \quad (2.1d) \\ y(0) = y_0, & \quad (2.1e) \end{cases}$$

where $\omega(\rho(t,y(t)+))$ denotes the right-hand limit of $\omega(\rho(t,x))$ at $x = y(t)$. Above, $\rho = \rho(t,x) \in [0,R]$ is the scalar conserved quantity and represents the traffic density, whose maximum attainable value is R. The flux function $f : [0,R] \to \mathbb{R}^+$ is assumed to be strictly concave and such that $f(0) = f(R) = 0$. In this paper, we will take $f(\rho) = \rho v(\rho)$, where $v(\rho) = V(1-\rho/R)$ is the mean traffic speed, V being the maximal velocity allowed on the road. The time-dependent variable y denotes the bus position. If the traffic is not too congested, the bus moves at its own maximal speed

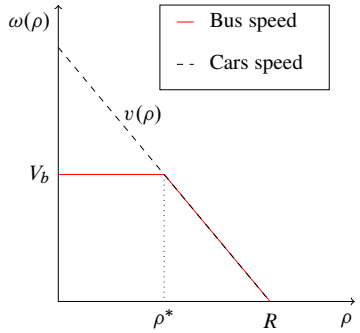

FIG. 1: Bus and cars speed

$V_b < V$. When the surrounding traffic density is too high, the bus adapts its velocity accordingly. In particular, it is not possible for the bus to overtake the cars. From a mathematical point of view, the velocity of the bus can be described by the traffic density dependent function (2.2) (see Figure 1)

$$\omega(\rho) = \begin{cases} V_b & \text{if } \rho \leqslant \rho^* \doteq R(1 - V_b/V), \\ v(\rho) & \text{otherwise.} \end{cases} \tag{2.2}$$

The bus acts as a moving obstacle, thus hindering the traffic flow as expressed by the flux constraint (2.1c). There, $\alpha \in]0, 1[$ is the dimensionless reduction rate of the road capacity at the bus position. The inequality (2.1c) is derived by studying the problem in the bus reference frame, i.e., setting $X = x - y(t)$ and rewriting the conservation law (2.1a) as

$$\partial_t \rho + \partial_X F(\rho) = 0, \qquad F(\rho) = f(\rho) - \dot{y}\rho. \tag{2.3}$$

Let $f_\alpha : [0, \alpha R] \to \mathbb{R}^+$ be the rescaled flux function describing the reduced flow at $x = y(t)$ (see the smaller curve in Figure 2a). It is possible to write explicitly the flux function for the reduced flux as $f_\alpha(\rho) = V\rho\left(1 - \frac{\rho}{\alpha R}\right)$. Moreover, let $\rho_\alpha \in]0, \alpha R/2[$ be defined as the density such that $F'_\alpha(\rho_\alpha) = 0 \Leftrightarrow f'_\alpha(\rho_\alpha) = \dot{y}$ with $F_\alpha(\rho) = f_\alpha(\rho) - \dot{y}\rho$, i.e. $\rho_\alpha = \frac{\alpha R}{2}\left(1 - \frac{\dot{y}}{V}\right)$, see Figure 2. Let us fix

$$F_\alpha = F_\alpha(\rho_\alpha) = f_\alpha(\rho_\alpha) - \dot{y}\rho_\alpha = \frac{\alpha R}{4V}\big(V - \dot{y}(t)\big)^2, \tag{2.4}$$

and imposing that in the bus reference frame the flux F should be less than the maximum value of the flux of the reduced flow, at the bus position one gets (2.1c). Note that the inequality is always satisfied if $\dot{y}(t) = v(\rho(t, y(t)))$, since the left-hand side is 0. Moreover, it is well defined even if ρ has a jump at $y(t)$ because of the Rankine–Hugoniot conditions. Following [21, Definition 4.1], solutions of (2.1) are defined as follows.

DEFINITION 2.1 A couple $(\rho, y) \in \mathcal{C}^0\left(\mathbb{R}^+; \mathbf{L^1} \cap \mathrm{BV}(\mathbb{R}; [0, R])\right) \times \mathbf{W^{1,1}}(\mathbb{R}^+; \mathbb{R})$ is a solution to (2.1) if

1. ρ is a weak solution of (2.1a), (2.1b), i.e., for all $\varphi \in \mathcal{C}^1_c(\mathbb{R}^2; \mathbb{R})$

$$\int_{\mathbb{R}^+}\int_{\mathbb{R}} \big(\rho\partial_t\varphi + f(\rho)\partial_x\varphi\big)dx\,dt + \int_{\mathbb{R}} \rho_o(x)\varphi(0, x)\,dx = 0\,; \tag{2.5a}$$

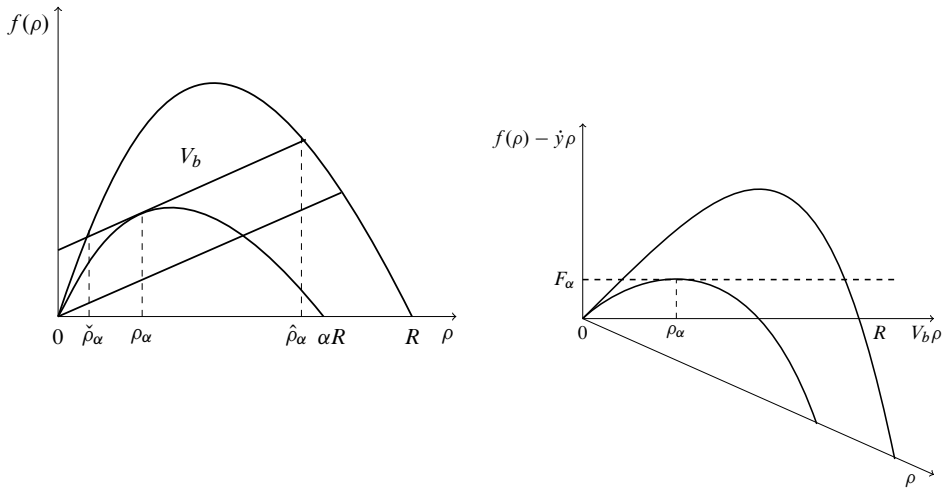

(a) Fixed reference frame (b) Bus reference frame

FIG. 2: Flux functions for $\dot{y} = V_b$. The small diagram represents the density-flux relation for the road with the reduced capacity.

moreover, ρ satisfies Kružhkov entropy conditions [30] on $\big(\mathbb{R}^+ \times \mathbb{R}\big) \setminus \big\{(t, y(t)) : t \in \mathbb{R}^+\big\}$, i.e., for every $k \in [0, R]$ and for all $\varphi \in \mathcal{C}_c^1(\mathbb{R}^2; \mathbb{R}^+)$ and $\varphi(t, y(t)) = 0$, $t > 0$,

$$\int_{\mathbb{R}^+} \int_{\mathbb{R}} \big(|\rho - k| \partial_t \varphi + \operatorname{sgn}(\rho - k) \big(f(\rho) - f(k) \big) \partial_x \varphi \big) \, dx \, dt + \int_{\mathbb{R}} |\rho_o - k| \varphi(0, x) \, dx \geqslant 0 \, ; \tag{2.5b}$$

2. y is a Carathéodory solution of (2.1d), (2.1e), i.e. for a.e. $t \in \mathbb{R}^+$

$$y(t) = y_o + \int_0^t \omega\big(\rho(s, y(s)+)\big) \, ds \, ; \tag{2.5c}$$

3. the constraint (2.1c) is satisfied, in the sense that for a.e. $t \in \mathbb{R}^+$

$$\lim_{x \to y(t)\pm} \big(f(\rho) - \omega(\rho)\rho \big)(t, x) \leqslant F_\alpha . \tag{2.5d}$$

with F_α defined in (2.4).

The existence of solutions for the general Cauchy problem with BV initial data is proved in [21]. Below, we specify how to construct the solution of a Riemann problem, as given by the definition of the Riemann Solver for problem (2.1) proposed in [21]. Let us consider a Riemann type initial datum

$$\rho_0(x) = \begin{cases} \rho_L & \text{if } x < 0, \\ \rho_R & \text{if } x > 0, \end{cases} \qquad y_0 = 0. \tag{2.6}$$

Denote by $\mathcal{R}$ the standard (i.e., without the constraint (2.1c)) Riemann solver for (2.1a)–(2.1b)–(2.6), i.e., the (right continuous) map $(t, x) \mapsto \mathcal{R}(\rho_L, \rho_R)(x/t)$ given by the standard weak entropy solution, see, for instance, [34].

DEFINITION 2.2 The standard Riemann solver $\mathcal{R} : [0, R]^2 \to \mathbf{L}^1_{\mathbf{loc}}(\mathbb{R}; [0, R])$ is defined as follows.

1. If $\rho_L < \rho_R$, then
$$\rho(t, x) = \begin{cases} \rho_L & \text{if } x < \lambda t, \\ \rho_R & \text{if } x \geqslant \lambda t, \end{cases}$$
2. If $\rho_L > \rho_R$, then
$$\rho(t, x) = \begin{cases} \rho_L & \text{if } x < f'(\rho_L)t, \\ f'^{-1}(\frac{x}{t}) & \text{if } f'(\rho_L)t < x < f'(\rho_R)t \\ \rho_R & \text{if } x \geqslant f'(\rho_R)t, \end{cases}$$

where $\lambda = \frac{(f(\rho_L)-f(\rho_R))}{(\rho_L-\rho_R)}$ is the speed of the jump given by the Rankine–Hugoniot condition. Moreover, let $\check{\rho}_\alpha$ and $\hat{\rho}_\alpha$, with $\check{\rho}_\alpha \leqslant \hat{\rho}_\alpha$, be the intersection points of the flux function $f(\rho)$ with the line $f_\alpha(\rho_\alpha) + V_b(\rho - \rho_\alpha)$ (see Figure 2(a)).

Following [20] we define the constrained Riemann Solver:

DEFINITION 2.3 The constrained Riemann solver $\mathcal{R}^\alpha : [0, R]^2 \to \mathbf{L}^1_{\mathbf{loc}}(\mathbb{R}; [0, R])$ is defined as follows.

1. If $f\big(\mathcal{R}(\rho_L, \rho_R)(V_b)\big) > F_\alpha + V_b\mathcal{R}(\rho_L, \rho_R)(V_b)$, then
$$\mathcal{R}^\alpha(\rho_L, \rho_R)(x/t) = \begin{cases} \mathcal{R}(\rho_L, \hat{\rho}_\alpha)(x/t) & \text{if } x < V_b t, \\ \mathcal{R}(\check{\rho}_\alpha, \rho_R)(x/t) & \text{if } x \geqslant V_b t, \end{cases} \quad \text{and} \quad y(t) = V_b t.$$
2. If $V_b\mathcal{R}(\rho_L, \rho_R)(V_b) \leqslant f\big(\mathcal{R}(\rho_L, \rho_R)(V_b)\big) \leqslant F_\alpha + V_b\mathcal{R}(\rho_L, \rho_R)(V_b)$, then
$$\mathcal{R}^\alpha(\rho_L, \rho_R) = \mathcal{R}(\rho_L, \rho_R) \quad \text{and} \quad y(t) = V_b t.$$
3. If $f\big(\mathcal{R}(\rho_L, \rho_R)(V_b)\big) < V_b\mathcal{R}(\rho_L, \rho_R)(V_b)$, i.e., $v\big(\mathcal{R}(\rho_L, \rho_R)(V_b)\big) < V_b$ then
$$\mathcal{R}^\alpha(\rho_L, \rho_R) = \mathcal{R}(\rho_L, \rho_R) \quad \text{and} \quad y(t) = v(\rho_R)t.$$

Note that, when the constraint is enforced (point 1. in the above definition), a non-classical shock arises between $\hat{\rho}_\alpha$ and $\check{\rho}_\alpha$, which satisfies the Rankine–Hugoniot condition but violates the Lax entropy condition, i.e., a discontinuity connecting two states ρ_L, ρ_R and traveling with speed λ given by the Rankine–Hugoniot relation is an entropy solution if and only if $f'(\rho_L) \geqslant \lambda \geqslant f'(\rho_R)$.

3. Numerical method

In this section, we aim at designing a numerical scheme for approximating the solutions of (2.1). The challenge is two-fold. First of all, we showed in the previous section that the constrained solutions contain non-classical shock waves violating the usual Lax entropy condition. It is now well-known that the numerical approximation of non-classical shock waves is a difficult task. The main reason for this is due to the numerical diffusion of the underlying numerical scheme which plays a crucial role and must be controlled to make the approximate and exact solutions coincide. Standard numerical schemes in general fail in this respect. We refer for instance the reader to [34, 35] and the references therein for a review, or [11] for a more recent work (see again the references therein).

Possible strategies to design relevant methods in this context are to consider either the so-called Glimm approaches [15, 27], or moving meshes. The idea behind these terminologies is to remove the numerical diffusion around the non-classical parts of the solutions either by sampling the (exact or approximate) Riemann solutions at each mesh interface for Glimm approaches, or by deforming the mesh cells in order for the mesh interfaces to follow the non-classical discontinuities. We refer for instance to [10, 12, 13, 20, 38]. The main drawbacks of these approaches are clearly the loss of conservation for the Glimm approaches and the laborious use of moving meshes.

In order to get rid of these two shortcomings, a new numerical approach was proposed in [7] to compute non-classical solutions to scalar conservation laws. The proposed scheme is fully conservative on fixed meshes and has the property of exactly capturing isolated non-classical shocks. For such isolated discontinuities it thus reduces at the minimum, namely at one point, the underlying numerical diffusion, unlike standard finite difference schemes. The method is based on an in-cell discontinuous reconstruction technique performed in each computational cell that may contain a non-classical shock. This section proposes to extend this approach to the present setting of a coupled PDE-ODE system in order to properly compute the non-classical shocks on a fixed mesh and to track at the same time the bus position.

Let Δx and Δt be the fixed space and time steps, and set $x_{j+1/2} = j\Delta x$, $x_j = (j - 1/2)\Delta x$ for $j \in \mathbb{Z}$ and $t^n = n\Delta t$ for $n \in \mathbb{N}$.

3.1 *Conservative scheme for hyperbolic PDEs with constraint*

In order to approximate the conservation law (2.1a), we place ourselves in the general framework of conservative finite volume schemes and first approximate the initial datum by a piecewise constant function given by its average on the discretization cells $C_j = [x_{j-\frac{1}{2}}, x_{j+\frac{1}{2}}[$, namely

$$\rho_j^0 = \frac{1}{\Delta x} \int_{x_{j-\frac{1}{2}}}^{x_{j+\frac{1}{2}}} \rho_0(x)dx, \quad j \in \mathbb{Z}.$$

As it is customary and in order to compute the approximation ρ_j^n of the average value of the exact solution ρ at time t^n on the cell C_j for $j \in \mathbb{Z}$ and $n \geqslant 1$, we then integrate the conservation law. Using Green's formula, we naturally end up with an iterative update procedure of the classical form

$$\rho_j^{n+1} = \rho_j^n - \frac{\Delta t}{\Delta x}\left(F_{j+\frac{1}{2}}^n - F_{j-\frac{1}{2}}^n\right), \tag{3.1}$$

where the numerical fluxes $F_{j+\frac{1}{2}}^n$ represent an approximate value of the exact flux that passes through the interface $x_{j+1/2}$ between the times t^n and t^{n+1}. In this case, the numerical fluxes $F_{j+\frac{1}{2}}^n$ have to be suitably defined at the cell interfaces $x_{j+\frac{1}{2}}$ in order to capture non-classical shocks.

Let us first notice that in the usual setting of classical solutions, a monotone and consistent numerical flux function like Godunov's can be used to define the numerical fluxes and provides reasonable first-order approximate solutions, see [28]. We will actually follow this approach away from the non-classical shocks, i.e., away from the bus position, and consider the Godunov's flux function [29] since the exact Riemann solution is known from the previous section. However, any flux function based on a consistent approximate Riemann solver could also be used at this stage without any restriction. In the vicinity of the bus position, namely where non-classical shock

waves may arise, we will follow the same approach as in [7] which consists in adding details in the piecewise constant representation (on each cell C_j) of the approximate solution. Recall indeed that classical finite volume schemes like Godunov's fail to generate good approximations of the exact solution in this case, see [7]. More precisely, we will reconstruct discontinuities in the relevant cells C_j and use them to define the numerical fluxes $F^n_{j+\frac{1}{2}}$ instead of simply using the constant values ρ^n_j and ρ^n_{j+1}. As we will see hereafter, such an approach will allow to *exactly* compute isolated non-classical discontinuities in the sense that for such solutions ρ^n_j will equal the average of the *exact* solution on the cell C_j. The corresponding numerical discontinuity will have numerical diffusion on one cell at most. Such a sharp control of the numerical diffusion is at the core of the success of the strategy to properly compute the non-classical discontinuities.

It is now a matter of defining which cell j is concerned with the reconstruction procedure, the reconstructed discontinuity itself, and the strategy to evaluate the numerical flux $F^n_{j+\frac{1}{2}}$ using the new details provided by the discontinuous reconstructions. We proceed as follows. Assume that at time t^n, the bus position y^n is located in the cell C_m for a given m. According to the Riemann solver provided in the previous section, a non-classical shock is expected to appear locally around the bus whenever the condition

$$f(\rho^n_m) > F_\alpha + V_b \rho^n_m, \tag{3.2}$$

is satisfied. In this case, the idea is to consider ρ^n_j not only as an approximation of the average value of the solution at time t^n on the cell C_j, but also as resulting from information on the structure of the exact Riemann solution $\mathcal{R}^\alpha(\rho^n_{m-1}, \rho^n_{m+1})$ associated with the states ρ^n_{m-1} and ρ^n_{m+1}. Therefore, if also

$$f\big(\mathcal{R}(\rho^n_{m-1}, \rho^n_{m+1})(V_b)\big) > F_\alpha + V_b \mathcal{R}(\rho^n_{m-1}, \rho^n_{m+1})(V_b), \tag{3.3}$$

holds, in the cell C_m we replace ρ^n_m by the left and right states $\rho^n_{m,l} = \hat{\rho}_\alpha$ and $\rho^n_{m,r} = \check{\rho}_\alpha$ corresponding to the non-classical shock appearing in the constrained Riemann solver associated with ρ^n_{m-1} and ρ^n_{m+1}. To guarantee mass conservation, the reconstructed discontinuity must be located inside C_m at the position

$$\bar{x}_m = x_{m-\frac{1}{2}} + d^n_m \Delta x, \tag{3.4}$$

where $d^m \in [0, 1]$ is defined by

$$d^n_m \rho^n_{m,l} + (1 - d^n_m)\rho^n_{m,r} = \rho^n_m, \tag{3.5}$$

or equivalently,

$$d^n_m = \frac{\rho^n_{m,r} - \rho^n_m}{\rho^n_{m,r} - \rho^n_{m,l}}, \tag{3.6}$$

see Figure 3. Remark that, due to (3.2), there holds $\check{\rho}_\alpha \leqslant \rho^n_m \leqslant \hat{\rho}_\alpha$, and therefore the condition $d^m \in [0, 1]$ is always satisfied.

To conclude the description of the reconstruction strategy, let us recall that the non-classical discontinuity moves with speed $V_b > 0$. It thus remains to define the numerical fluxes.

Let us first recall that Godunov's flux function (or any monotone and consistent numerical flux) is used to define $F^n_{j+1/2}$, $j \neq m$, under the classical CFL condition

$$\Delta t \max_{j\in\mathbb{Z}} \big|f'(\rho^n_j)\big| \leqslant \frac{1}{2}\Delta x, \tag{3.7}$$

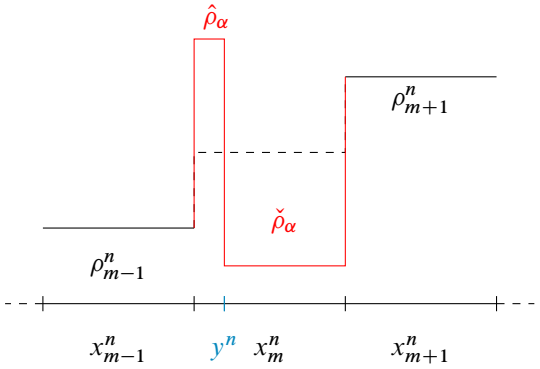

FIG. 3: Reconstruction of a non-classical shock

and we keep the same definition for $F^n_{m+1/2}$ whenever the conditions (3.2) and (3.3) are not both satisfied simultaneously. Thus we only need to define $F^n_{m+1/2}$ when (3.2) and (3.3) hold. Since $V_b > 0$, all the waves in the Riemann solution $\mathcal{R}(\rho^n_{m,r}, \rho^n_{m+1})$ associated with the initial states $\rho^n_{m,r}$ and ρ^n_{m+1} also have positive speed. As a consequence, we can define the numerical flux $F^n_{m+1/2}$ using the reconstructed discontinuity in the cell C_j and considering that the numerical flux equals the exact flux evaluated on the right state $\rho^n_{m,r}$ until the reconstructed discontinuity reaches the interface $x_{j+1/2}$, and the exact flux evaluated on the left state $\rho^n_{m,l}$ afterwards. More precisely, if we denote

$$\Delta t_{m+\frac{1}{2}} = \frac{1-d^n_m}{V_b}\Delta x$$

the time needed by the reconstructed discontinuity to reach the interface, the definition of the numerical flux at $x_{m+\frac{1}{2}}$ is given by

$$\Delta t\, F^n_{m+\frac{1}{2}} = \min\left(\Delta t_{m+\frac{1}{2}}, \Delta t\right) f(\rho^n_{m,r}) + \max\left(\Delta t - \Delta t_{m+\frac{1}{2}}, 0\right) f(\rho^n_{m,l}). \tag{3.8}$$

Following [7], let us prove that isolated non-classical shocks are exactly captured with our strategy (see also Case 0 in Section 4 below for a numerical illustration) and contain no spurious numerical diffusion.

DEFINITION 3.1 We define the exact numerical solution on each cell C_j as

$$\rho^n_j = \frac{1}{\Delta x}\int_{x_{j-1/2}}^{x_{j+1/2}} \rho(x, t^n)dx, \qquad j \in \mathbb{Z},\ n \in \mathbb{N}, \tag{3.9}$$

where $(x,t) \to \rho(x,t)$ denotes the exact Riemann solution of the coupled PDE-ODE problem given by $\rho(x,t) = \hat{\rho}_\alpha$ if $x < V_b t$ and $\rho(x,t) = \check{\rho}_\alpha$ otherwise.

Theorem 3.2 *Assume that $\rho_{0,j} = \hat{\rho}_\alpha$ if $j \leqslant 0$ and $\rho_{0,j} = \check{\rho}_\alpha$ if $j \geqslant 1$ and that the bus initial position is $y_0 = 0$. Then the proposed conservative scheme provides an exact numerical solution in the sense of Definition 3.1. In particular, the numerical discontinuity is diffused on one cell at most.*

Proof. Let us first notice that there is no relevant reconstruction in the first time iteration. Indeed, since $y_0 = 0$ the bus is located in cell C_1 and (3.6) gives $d^0_1 = 0$. As a consequence, the only

possible reconstruction turns out to be trivial in the sense that we recover $\check{\rho}_\alpha$ in the whole cell C_1. After one time step Δt, the exact solution given by $\rho(x, \Delta t) = \hat{\rho}_\alpha$ if $x < V_b \Delta t$ and $\rho(x, \Delta t) = \check{\rho}_\alpha$ otherwise is such that

$$\frac{1}{\Delta x}\int_{x_{j-1/2}}^{x_{j+1/2}} \rho(x, \Delta t)dx = \begin{cases} \hat{\rho}_\alpha & \text{if} \quad j \leqslant 0, \\ \check{\rho}_\alpha - V_b \dfrac{\Delta t}{\Delta x}(\check{\rho}_\alpha - \hat{\rho}_\alpha) & \text{if} \quad j = 1, \\ \check{\rho}_\alpha & \text{if} \quad j > 1. \end{cases} \tag{3.10}$$

But recall that by definition of $\check{\rho}_\alpha$ and $\hat{\rho}_\alpha$ we have $f(\check{\rho}_\alpha) - f(\hat{\rho}_\alpha) = V_b(\check{\rho}_\alpha - \hat{\rho}_\alpha)$ so that we also have

$$\frac{1}{\Delta x}\int_{x_{j-1/2}}^{x_{j+1/2}} \rho(x, \Delta t)dx = \begin{cases} \hat{\rho}_\alpha - \dfrac{\Delta t}{\Delta x}\big(f(\hat{\rho}_\alpha) - f(\hat{\rho}_\alpha)\big) & \text{if} \quad j \leqslant 0, \\ \check{\rho}_\alpha - \dfrac{\Delta t}{\Delta x}\big(f(\check{\rho}_\alpha) - f(\hat{\rho}_\alpha)\big) & \text{if} \quad j = 1, \\ \check{\rho}_\alpha - \dfrac{\Delta t}{\Delta x}\big(f(\check{\rho}_\alpha) - f(\check{\rho}_\alpha)\big) & \text{if} \quad j > 1, \end{cases} \tag{3.11}$$

that is to say, under the CFL restriction (3.7),

$$\rho_j^1 = \frac{1}{\Delta x}\int_{x_{j-1/2}}^{x_{j+1/2}} \rho(x, \Delta t)dx, \qquad j \in \mathbb{Z}. \tag{3.12}$$

Equality (3.9) is then proved for the first iterate.

Interestingly, by conservation the reconstructed discontinuity is necessarily located at the exact position of the solution, namely at the bus position $x = V_b \Delta t$. In other words, we reconstruct the exact solution at time $t = \Delta t$. To get the required identity (3.9) for the second iterate, it is sufficient to notice that since the proposed definition of the numerical flux $F^1_{1+1/2}$ is exact and based on the reconstructed discontinuity, all the numerical fluxes $F^1_{j+1/2}$ are in fact exact (the other fluxes $F^1_{j+1/2}$, $j \neq 1$ are also exact by consistency since the left and right states ρ^1_j and ρ^1_{j+1} are the same and equal to $\hat{\rho}_\alpha$ or $\check{\rho}_\alpha$). Thus, by Green's formula, the updated values on each cell will coincide again with the average value of the exact solution on the cell. And the process is going on in a similar way for the next time iterations, which proves the result. □

Again, this result proves that the proposed strategy allows to control the numerical diffusion associated with the non-classical shocks. It is reduced at the minimum and non-classical discontinuities are thus properly computed. Notice that at this stage, classical shocks still suffer some numerical diffusion since classical Godunov's method is used away from the bus position. In practice, we observed that this might be problematic in the validation of the solution on the constraint (3.3). In fact, if we choose initial data in the neighborhoods of the values $\hat{\rho}_\alpha$, $\check{\rho}_\alpha$, we observe that the approximate solution generated by this method may be not correct because of the numerical diffusion. To overcome this problem, we propose to apply the reconstruction technique also to classical shocks, in order to exactly control the numerical diffusion. To show why this is necessary let us suppose to have the following initial data:

$$\rho_0(x) = \begin{cases} \check{\rho}_\alpha - \varepsilon & \text{if } x < 0.5, \\ \hat{\rho}_\alpha + \varepsilon & \text{if } x > 0.5, \end{cases} \tag{3.13}$$

where $\varepsilon = 10^-4$. The exact solution to correspondent Riemann problem is a classical shock with $\rho_l = \check{\rho}_\alpha - \varepsilon$ and $rho_r = \hat{\rho}_\alpha - \varepsilon$. However, when this problem is solved numerically due to the

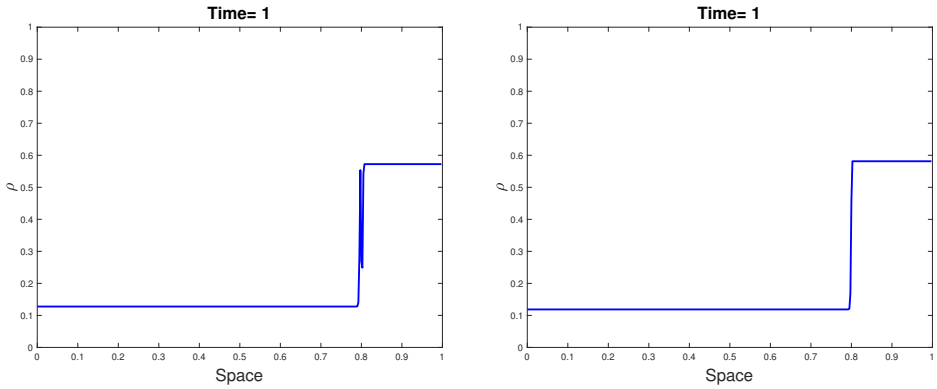

(a) Shock without reconstruction (b) Shock with reconstruction

FIG. 4: Numerical solution in the case of initial data as in 3.13

numerical diffusion the numerical solution will generate non-classical behavior, see Figure 4. In the spirit of [31] and following the same lines as above, we proceed as follows. Let us first recall that, due to the entropy condition, the left trace value of a classical shock is always smaller than the right one. Given a cell C_j for some $j \in \mathbb{Z}$, $j \neq m$, such that $\rho^n_{j-1} < \rho^n_{j+1}$, we introduce the left and right traces $\rho^n_{j,l} = \rho^n_{j-1}$ and $\rho^n_{j,r} = \rho^n_{j+1}$ of a reconstructed discontinuity and we define d^n_j by

$$d^n_j = \frac{\rho^n_{j,r} - \rho^n_j}{\rho^n_{j,r} - \rho^n_{j,l}}. \tag{3.14}$$

Let us denote by $\lambda(\rho^n_{j,l}, \rho^n_{j,r})$ the speed of the discontinuity given by the Rankine–Hugoniot condition, i.e.,

$$\lambda(\rho^n_{j,l}, \rho^n_{j,r}) = \frac{f(\rho^n_{j,l}) - f(\rho^n_{j,r})}{\rho^n_{j,l} - \rho^n_{j,r}}.$$

Then, if it is actually possible to reconstruct such a discontinuity within the cell C_j, that is to say if $d^n_j \in [0, 1]$, the numerical fluxes at $x_{j\pm\frac{1}{2}}$ are defined by

- if $\lambda(\rho^n_{j,l}, \rho^n_{j,r}) \geqslant 0$,

$$\Delta t\, F^n_{j+\frac{1}{2}} = \min\left(\Delta t_{j+\frac{1}{2}}, \Delta t\right) f(\rho^n_{j,r}) + \max\left(\Delta t - \Delta t_{j+\frac{1}{2}}, 0\right) f(\rho^n_{j,l}), \tag{3.15}$$

  with $\Delta t_{j+\frac{1}{2}} = \dfrac{1 - d^n_j}{\lambda(\rho^n_{j,l}, \rho^n_{j,r})} \Delta x.$

- if $\lambda(\rho^n_{j,l}, \rho^n_{j,r}) \leqslant 0$,

$$\Delta t\, F^n_{j-\frac{1}{2}} = \min\left(\Delta t_{j-\frac{1}{2}}, \Delta t\right) f(\rho^n_{j,l}) + \max\left(\Delta t - \Delta t_{j-\frac{1}{2}}, 0\right) f(\rho^n_{j,r}), \tag{3.16}$$

  with $\Delta t_{j-\frac{1}{2}} = \dfrac{d^n_j}{-\lambda(\rho^n_{j,l}, \rho^n_{j,r})} \Delta x,$

where, with some abuse of notation, we mean that if $\lambda(\rho^n_{j,l}, \rho^n_{j,r}) = 0$ then $F^n_{j+\frac{1}{2}} = f(\rho^n_{j,r})$ and $F^n_{j-\frac{1}{2}} = f(\rho^n_{j,l})$. This additional reconstruction guarantees that also isolated classical shocks are exactly captured (the same theorem as above can be stated and proved in the same way), as illustrated by the numerical tests presented in Section 4. Moreover, with this supplementary reconstruction we are able to handle correctly all the interactions among shocks, both classical and non-classical.

REMARK 3.3 In the event of an ambiguity, for instance $j = m + 1$ and $\lambda \leqslant 0$ above, the priority is given to the reconstruction of the non-classical discontinuity.

3.2 *Numerical method for the ODE*

To precisely track the bus trajectory we adapt the algorithm introduced in [9]. At each time step, we update the position y^n of the bus by studying interactions between the bus trajectory and the density waves within the corresponding cell. We distinguish two cases:

1. Inequality (3.2) is satisfied. Then the bus moves at velocity V_b and we update the bus position as $y^{n+1} = V_b \Delta t^n + y^n$.
2. Condition (3.2) is not satisfied. In this case the solution is classical and we implement the tracking algorithm introduced in [9]. We have to distinguish two situations: one when $y^n \in [x_{m-\frac{1}{2}}, x^n_m[$ and one when $y^n \in [x^n_m, x_{m+\frac{1}{2}}[$. If no interaction occurs between the wave originating at the corresponding cell interface and the bus in Δt^n, the ODE is solved by

$$y^{n+1} = y^n + \omega(\rho^n_m)\Delta t.$$

Otherwise, we check if the wave is a shock or a rarefaction:

- The wave is a shock: We compute the incremental interaction time $\bar{t}$ and the bus trajectory is given by
$$y^{n+1} = y^n + \omega(\rho^n_m)\bar{t} + \omega(\rho^n_{m\pm1})(\Delta t - \bar{t}).$$
- The wave is a rarefaction: First of all, we observe that if this wave originated at $x_{m-\frac{1}{2}}$ and an interaction occurs, the bus must travel at its maximal velocity V_b, and it will keep this velocity, as in Case 1. Therefore, we focus on the case of a rarefaction originating at $x_{m+\frac{1}{2}}$. We still note that, if the bus is initially travelling at speed V_b, it will keep this velocity after the interaction, see Case 1. When the bus does not travel at the constant speed V_b, then we need to compute the first and last interaction points with the bus trajectory, respectively $(\bar{t}, \bar{x})$ and $(\bar{\bar{t}}, \bar{\bar{x}})$ such that we can know the exact bus speed and hence, its position. Then:
  - If $\bar{\bar{t}} \geqslant \Delta t$ the new position is given by $y^{n+1} = \tilde{y}(\Delta t)$ with $\tilde{y}(\Delta t)$ being given by
$$\tilde{y}(t) = x_{m+\frac{1}{2}} + (t - t^n) - \sqrt{t - t^n}\left(\frac{\bar{t} - t^n + x_{m+\frac{1}{2}} - \bar{x}}{\sqrt{\bar{t} - t^n}}\right)$$
  - If $\bar{\bar{t}} < \Delta t$ then $y^{n+1} = \tilde{y}(\bar{\bar{t}}) + (\Delta t - \bar{\bar{t}})\omega(\rho^n_{m+1})$

The cell index m is then updated according to the new position of the bus.

4. Numerical results

In this section we present some numerical tests performed with the scheme previously described. We deal with a road of length 1 parameterized by the interval $[0, 1]$. In all the simulations we fix $V_b = 0.3, \alpha = 0.6, V = R = 1$.

Case 0: We consider Riemann type initial data with

$$\rho_0(x) = \begin{cases} \hat{\rho}_\alpha & \text{if } x < 0.5, \\ \check{\rho}_\alpha & \text{if } x > 0.5, \end{cases} \qquad y_0 = 0.5. \tag{4.1}$$

The solution is given by a non-classical shock, as illustrated in Figure 5. It is possible to notice in this case that the numerical solution is exact everywhere but in the single cell containing the non-classical shock. However, as already said, the value in this cell coincides with the average of the corresponding exact solution and using (3.6) we can recover the exact location of the discontinuity.

Case I: We consider Riemann type initial data with

$$\rho_0(x) = \begin{cases} 0.4 & \text{if } x < 0.5, \\ 0.5 & \text{if } x > 0.5, \end{cases} \qquad y_0 = 0.5. \tag{4.2}$$

The solution is given by two classical shocks separated by a non-classical discontinuity, as illustrated in Figure 6, left.

Case II: We consider Riemann type initial data with

$$\rho_0(x) = \begin{cases} 0.8 & \text{if } x < 0.5, \\ 0.5 & \text{if } x > 0.5, \end{cases} \qquad y_0 = 0.5. \tag{4.3}$$

The values of the initial conditions create a rarefaction wave followed by non-classical and classical shocks, as illustrated in Figure 6, right.

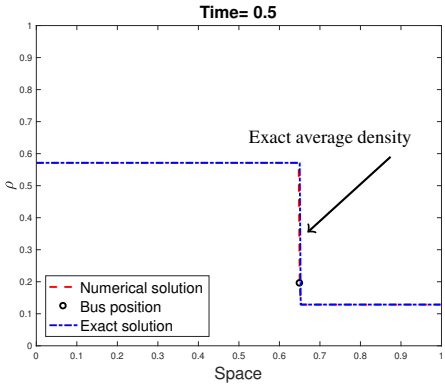

FIG. 5: Evolution in time of the density corresponding to initial data (4.1) (left) with $\Delta x = 0.001$ compared with the exact solution

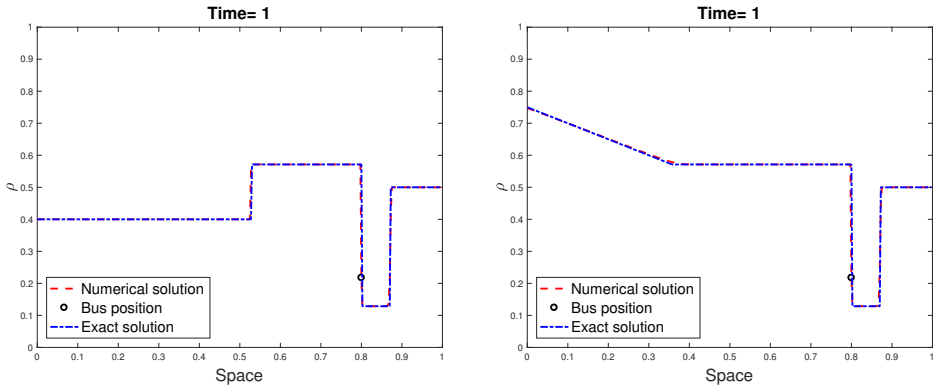

FIG. 6: Evolution in time of the density corresponding to initial data (4.2) (left) and (4.3) (right) with $\Delta x = 0.001$ compared with the exact solution

Case III: We consider the following initial data

$$\rho_0(x) = \begin{cases} 0.8 & \text{if } x < 0.5, \\ 0.5 & \text{if } x > 0.5, \end{cases} \qquad y_0 = 0.4. \tag{4.4}$$

In this case, the bus initial position is not aligned with the discontinuity. We can see that the values of the initial conditions generate a rarefaction wave followed by non-classical and classical shocks on the density that are created when the bus approaches the rarefaction and initiates a moving bottleneck, as illustrated in Figure 7.

Case IV: We consider the following initial data

$$\rho_0(x) = \begin{cases} \hat{\rho}_\alpha & \text{if } x < 0.25, \\ \check{\rho}_\alpha & \text{if } 0.25 < x < 0.5, \\ 0.95 & \text{if } x > 0.5, \end{cases} \qquad y_0 = 0.25. \tag{4.5}$$

The solution is given by a non-classical shock and a classical one that collide. After the collision a classical shock is generated, as illustrated in Figure 8.

For completeness, we show the $x-t$ plots for the differentes in Figure 9 which allows to follow the complete bus trajectory at each time step.

For cases I and II we also show the convergence curves in Figure 10. It represents the log-log $\mathbf{L^1}$ error between the numerical solution and the exact one versus mesh size. The numerical order of convergence can be found in Table 1.

5. Conclusions

In this paper, we introduced a reconstruction based numerical method that is able to capture numerically non-classical shocks for a coupled PDE-ODE problem with moving constraints. The algorithm is conservative on a fixed mesh and isolated classical and non-classical shocks are

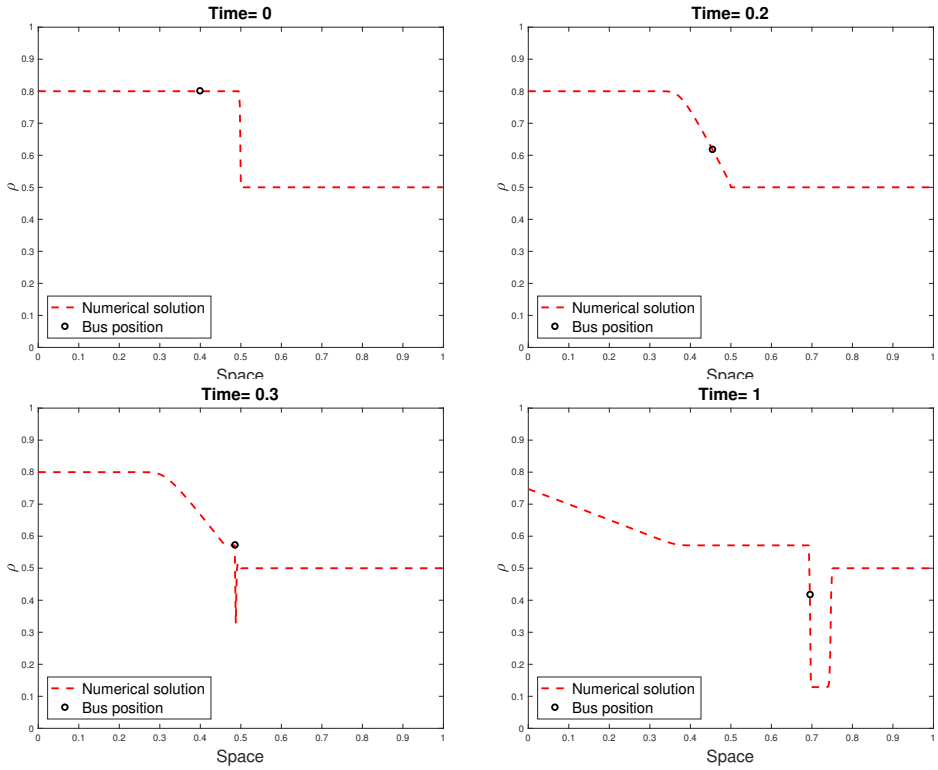

FIG. 7: Evolution in time of the density at different times corresponding to initial data (4.4) and $\Delta x = 0.001$

propagated exactly. We showed several test cases, including shock interactions and tests that are more significant from a modeling point of view. The convergence of the method was shown numerically.

TABLE 1: Order of convergence for the reconstruction scheme, corresponding to initial data (4.2) and (4.3)

Δx	Order of convergence for Case I	Order of convergence for Case II
0.1	1.1762	0.8212
0.05	0.9928	0.8794
0.025	1.1360	0.9494
0.0125	1.5980	1.4522
0.00625	0.7769	1.0049
0.003125	0.8473	1.0103
0.0015625	0.8871	1.1898

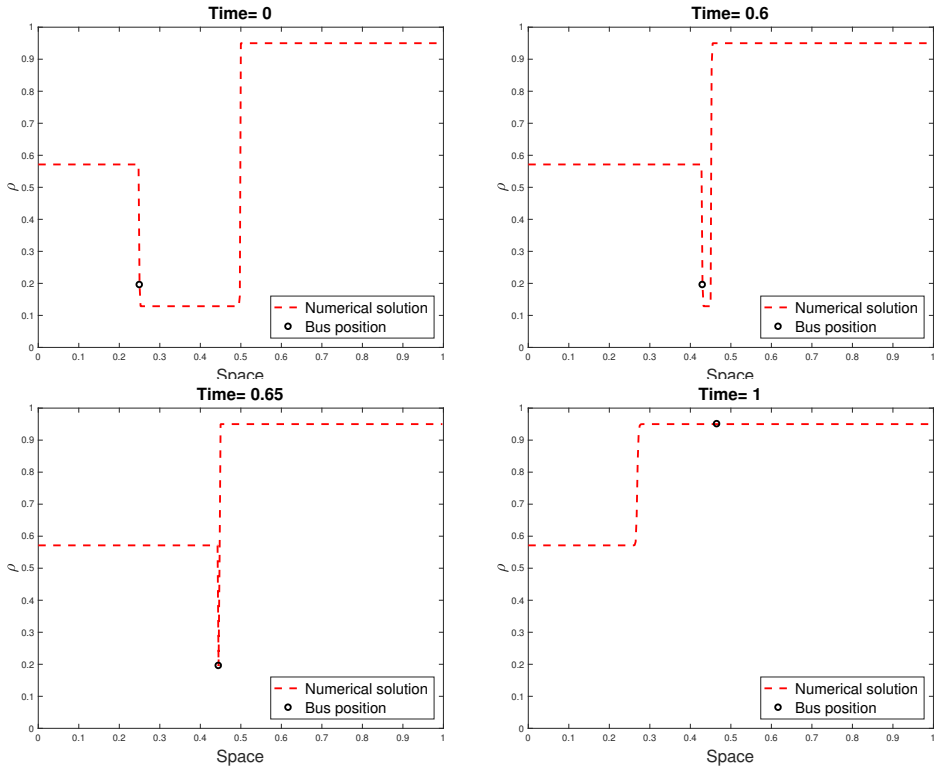

FIG. 8: Evolution in time of the density at different times corresponding to initial data (4.5) and $\Delta x = 0.001$

Acknowledgments. This research was supported by the European Research Council under the European Union's Seventh Framework Program (FP/2007–2013)/ERC Grant Agreement n. 257661.

References

1. Aguillon, N., A non-dissipative reconstruction scheme for the compressible Euler equations. arXiv:1403.7497 (2014).
2. Aguillon, N., Capturing nonclassical shocks in nonlinear elastodynamic with a conservative finite volume scheme. *Interfaces Free Bound.* **18** (2016), 137–159. Zbl06655298 MR3549004
3. Aguillon, N. & Chalons, C., Non diffusive conservative schemes based on approximate Riemann solvers for Lagrangian gas dynamics. *ESAIM, Math. Model. Numer. Anal.* **50** (2016), 1887–1916. Zbl06669878 MR3580126
4. Andreianov, B., Goatin, P. & Seguin, N., Finite volume schemes for locally constrained conservation laws. *Numer. Math.*, **115** (2010), 609–645. With supplementary material available online. Zbl1196.65151 MR2658157
5. Borsche, R., Colombo, R. & Garavello, M., Mixed systems: ODEs-balance laws. *Journal of Differential equations* **252** (2012), 2311–2338. Zbl1252.35193 MR2860620

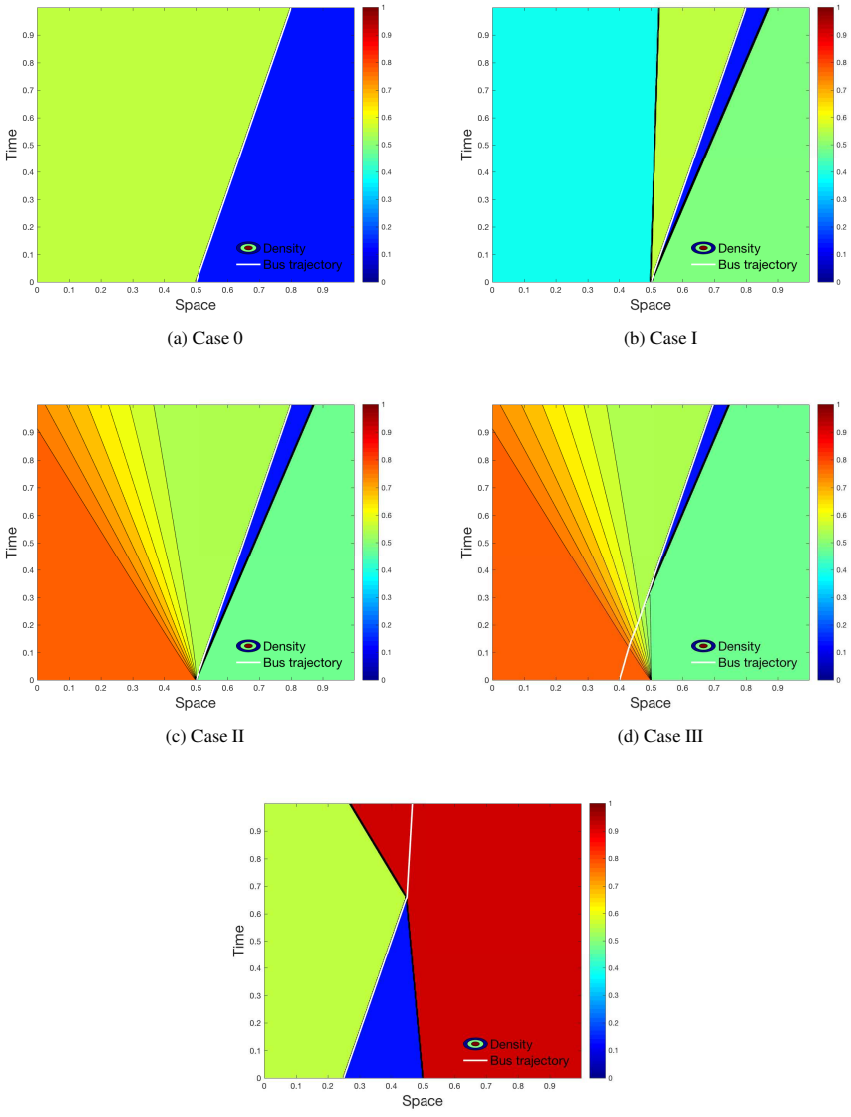

(a) Case 0

(b) Case I

(c) Case II

(d) Case III

(e) Case IV

FIG. 9: $x - t$ plots for the different cases

6. Borsche, R., Colombo, R. M. & Garavello, M., On the coupling of systems of hyperbolic conservation laws with ordinary differential equations. *Nonlinearity* **23** (2010), 2749–2770. Zbl1205.35170 MR2727168
7. Boutin, B., Chalons, C., Lagoutière, F. & LeFloch, P. G., Convergent and conservative schemes for nonclassical solutions based on kinetic relations. I. *Interfaces and Free Boundaries* **10** (2008), 399–421. Zbl1157.65435 MR2453138

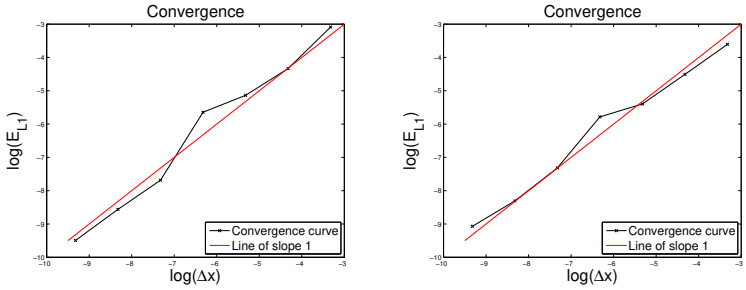

(a) Classical and non-classical shock – Case I (b) Rarefaction and non-classical shock – Case II

FIG. 10: $\mathbf{L^1}$ convergence

8. Bressan, A., *Hyperbolic Systems of Conservation Laws*, volume 20 of Oxford Lecture Series in Mathematics and its Applications. Oxford University Press, Oxford, (2000). Zbl0997.35002 MR1816648
9. Bretti, G. & Piccoli, B., A tracking algorithm for car paths on road networks. *SIAM Journal on Applied Dynamical Systems* **7** (2008), 510–531. Zbl1168.35389 MR2421115
10. Chalons, C., Numerical approximation of a macroscopic model of pedestrian flows. *SIAM J. Sci. Comput.* **29** (2007), 539–555. Zbl1143.35339 MR2306257
11. Chalons, C., Engel, P. & Rohde, C., A conservative and convergent scheme for undercompressive shock waves. *SIAM J. Numer. Anal.* **52** (2014), 554–579. Zbl 06296654 MR3168613
12. Chalons, C. & Goatin, P., Transport-equilibrium schemes for computing contact discontinuities in traffic flow modeling. *Commun. Math. Sci.* **3** (2007), 533–551. Zbl1141.35412 MR2352330
13. Chalons, C. & Goatin, P., Godunov scheme and sampling technique for computing phase transitions in traffic flow modeling. *Interfaces and Free Boundaries* **10** (2008), 197–221. Zbl1171.35429 MR2453129
14. Chalons, C., Goatin, P. & Seguin, N., General constrained conservation laws. Application to pedestrian flow modeling. *Netw. Heterog. Media* **8** (2013), 433–463. Zbl1275.35144 MR3063560
15. Colella, P., Glimm's method for gas dynamics. *SIAM J. Sci. Stat. Comput.* **3** (1982), 76–110. Zbl0502.76073 MR0651869
16. Colombo, R. M. & Goatin, P., A well posed conservation law with a variable unilateral constraint. *J. Differential Equations* **234** (2007), 654–675. Zbl1116.35087 MR2300671
17. Colombo, R. M. & Marson, A., A Hölder continuous ODE related to traffic flow. *Proc. Roy. Soc. Edinburgh Sect. A* **133**, (2003), 759–772. Zbl1052.34007 MR2006201
18. Daganzo, C. & Laval, J. A., Moving bottlenecks: A numerical method that converges in flows. *Transportation Research Part B* **39** (2005), 855–863.
19. Daganzo, C. & Laval, J. A., On the numerical treatement of moving bottlenecks. *Transportation Research Part B* **39** (2005), 31–46.
20. Delle Monache, M. L. & Goatin, P., A front tracking method for a strongly coupled PDE-ODE system with moving density constraints in traffic flow. *Discrete Contin. Dyn. Syst. Ser. S* **7** (2014), 435–447. Zbl1292.90078 MR3177727
21. Delle Monache, M. L. & Goatin, P., Scalar conservation laws with moving constraints arising in traffic flow modeling: An existence result. *J. Differential Equations* **257** (2014), 4015–4029. Zbl1302.35248 MR3264413
22. Filippov, V. V., *Ordinary Differential Equations With Discontinuous Right-hand Sides*, volume 30. Kluwer Academic Publishers (1994). Zbl0852.34004 MR1334843

23. Garavello, M. & Goatin, P., The Aw-Rascle traffic model with locally constrained flow. *J. Math. Anal. Appl.* **378** (2011), 634–648. Zbl1211.35018 MR2773272
24. Garavello, M. & Piccoli, B., *Traffic Flow on Networks*, volume 1 of AIMS Series on Applied Mathematics. American Institute of Mathematical Sciences (AIMS), Springfield, MO, (2006). Zbl1136.90012 MR2328174
25. Gasser, I., Lattanzio, C. & Maurizi, A., Vehicular traffic flow dynamics on a bus route. *Multiscale Model. Simul.* **11** (2013), 925–942. Zbl1282.35238 MR3103240
26. Giorgi, F., Prise en compte des transports en commun de surface dans la modélisation macroscopique de l'écoulement du trafic. PhD thesis, Institut National des Sciences Appliquées de Lyon (2002).
27. Glimm, J., Solutions in the large time for non-linear hyperbolic systems of equations. *Comm. Pure Appl. Math.* **18** (1965), 697–715. Zbl0141.28902 MR0194770
28. Godlewski, E. & Raviart, P.-A., *Numerical Approximation of Hyperbolic Systems of Conservation Laws*. Applied Mathematical Sciences, 118. Springer-Verlag, New York, 1996. Zbl0860.65075 MR1410987
29. Godunov, S. K., A finite difference method for the numerical computation of discontinuous solutions of the equations of fluid dynamics. *Matematicheskii Sbornik* **47** (1959), 271–290.
30. Kružhkov, S. N., First order quasilinear equations with several independent variables. *Mat. Sb. (N.S.)* **81** (1970), 228–255. Zbl0202.11203 MR0267257
31. Lagoutière, F., Stability of reconstruction schemes for scalar hyperbolic conservation laws. *Communication in Mathematical Sciences* **6** (2008), 57–70. Zbl1140.35325 MR2397997
32. Lattanzio, C., Maurizi, A. & Piccoli, B., Moving bottlenecks in car traffic flow: A PDE-ODE coupled model. *SIAM J. Math. Anal.* **43** (2011), 50–67. Zbl1227.35206 MR2765683
33. Lebacque, J.-P., Lesort, J. B. & Giorgi, F., Introducing buses into first-order macroscopic traffic flow models. *Transportation Reasearch Record* **1644** (1998), 70–79.
34. LeFloch, P. G., *Hyperbolic Systems of Conservation Laws: The Theory of Classical and Nonclassical Shock Waves*. Lecture Notes in Mathematics, ETH Zurich, Birkhauser, (2002). Zbl1019.35001
35. LeFloch, P. G., Kinetic relations for undercompressive shock waves. Physical, mathematical, and numerical issues. In: *Nonlinear Partial Differential Equations and Hyperbolic Wave Phenomena*, volume 526 of Contemp. Math., Amer. Math. Soc., Providence, RI, (2010), 237–272. Zbl1221.35235 MR2731995
36. Lighthill, M. J. & Whitham, G. B., On kinematic waves. II. A theory of traffic flow on long crowded roads. *Proc. Roy. Soc. London Ser. A* **229** (1955), 317–346. Zbl0064.20906 MR0072606
37. Richards, P. I., Shock waves on the highway. *Operations Research* **4** (1956), 42–51. MR0075522
38. Zhong, X., Hou, T. Y. & LeFloch, P. G., Computational methods for propagating phase boundaries. *J. Comput. Phys.* **124** (1996), 192–216. MR1378558